THE GRAVITATIONAL COLLAPSE OF IRON–OXYGEN STARS WITH MASSES OF 2 $M_\odot$ AND 10 $M_\odot$

II

D. K. NADYOZHIN

Institute of Applied Mathematics, U.S.S.R., Academy of Sciences, Moscow, U.S.S.R.

(Received 22 February, 1977)

Abstract. The collapse of iron–oxygen stars with masses of 2 $M_\odot$ has been calculated. The commencement of the collapse is due to dissociation of iron-group nuclei into free nucleons. After a while, the collapse proceeds in consequence of intensive energy losses due to neutrino volume radiation. At an intermediate stage of the collapse, the core – opaque with respect to neutrino radiation (neutrino core) – is formed inside the collapsing star. Both the gradual increase of the mass of the neutrino core and the partial absorption of neutrinos radiated from the surface of the neutrino core by the stellar envelope (deposition) were taken into account in our calculations. The kinetics of oxygen burning in the outer layers of the envelope was also allowed for. Neither the deposition, nor the oxygen burning, result in ejection of stellar envelopes.

1. Introduction

This paper deals with the calculations of the gravitational collapse of iron–oxygen stars of masses 2 $M_\odot$ and 10 $M_\odot$. The relevant equations and the calculating formulae were discussed by Nadyozhin (1975) (hereafter referred to as NI). We shall discuss here mainly the hydrodynamics of the collapse, which can be divided into two substantially different stages (NI): (a) an initial *transparent* stage, which proceeds in the regime of volume neutrino energy losses and (b) a final *opaque* stage, which is characterized by intensive neutrino and antineutrino energy losses from the surface of the opaque (for neutrinos and antineutrinos) stellar core (or 'neutrino core' hereafter for simplicity). A short intermediate *semi-transparent* stage ensures a smooth transition from the transparent stage to the opaque one.

2. The Transparent Stage of the Collapse

Figure 1 shows the $T\varrho$-diagram for the transparent stage of the collapse of 2 $M_\odot$ iron–oxygen star. The symbols $*$ and ● denote the stellar centre and surface, respectively. The curves in Figures 1–6 are labeled with integers related to successive moments of time in accordance with Table I. The number 0 corresponds to stellar structure when 1000 time steps are calculated. The structure of the star at this moment is practically indistinguishable from the initial polytropic model of index $n=3$. It should be noted that the internal structure of the initial model is not generally represented by a straight line in the (log T, log ϱ)-plane, since the initial distribution of temperature is calculated from the relation $P \sim \varrho^{4/3}$ with rather a complex dependence of P on T and ϱ allowing

Astrophysics and Space Science **51** (1977) 283–301.

for electron degeneracy and dissociation of iron-group nuclei (NI). According to Table I, it takes the star about 15 s (the first 15 000 calculated steps) to pass into the state of rapid gravitational collapse. During this transition the star pulsates in the fundamental mode (cf. the positions of the stellar surface in Figure 1 at moments 0, 1 and 2). The local bends of the curves in Figure 1 at $\varrho \approx 10^7$ g cm^{-3} are due to oxygen burning by the reaction $O^{16}+O^{16}$. The oxygen envelope is situated below and iron core above these bends.

TABLE I

The moments of time for Figures 1–6. (The time is measured from the moment when the mean neutrino-antineutrino 'optical' depth of the star, τ_ν, equals to 0.001)

The integers labeling the curves in Figures 1–6	The number of calculated time steps	Time in seconds
0	1 000	−15.0
1	15 000	−0.624
2	16 100	−0.062 7
3	16 300	−0.018 9
4	16 400	−0.005 22
5	16 500	+0.001 34
6	16 600	+0.001 91

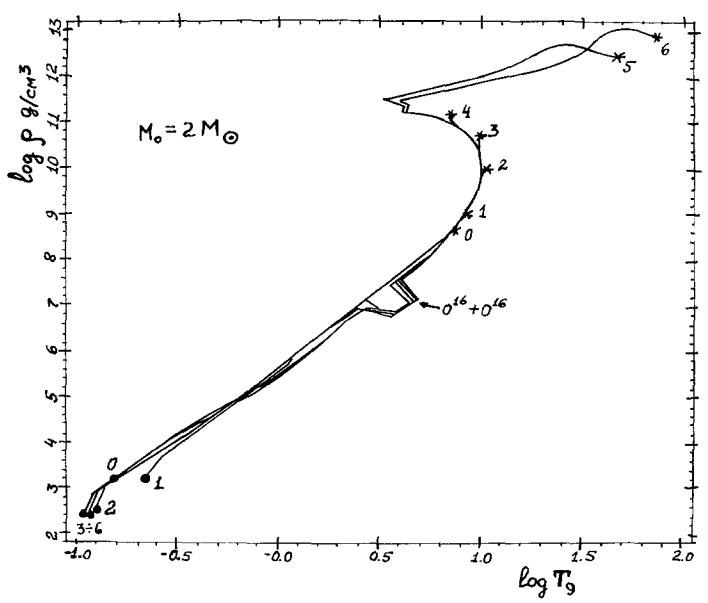

Fig. 1. Temperature-density diagram. The moments of time corresponding to integers 0–6 are presented in Table I. Marker * stands for stellar centre, marker ● – for stellar surface.

Figures 2–5 show the distributions of temperature, density, Eulerian radius, and velocity over Lagrangian coordinate J, which is taken to be equal to the mesh point number. The relation between J and mass-coordinate m is shown under horizontal axis in Figure 2 (a more detailed relation is given in Table III in NI). At the stellar centre, $J=1$; and at the surface, $J=151$. Only the internal part (up to $J=130$) of the collapsing star is shown in Figures 2–5; the oxygen envelope being situated at $J=136$–151.

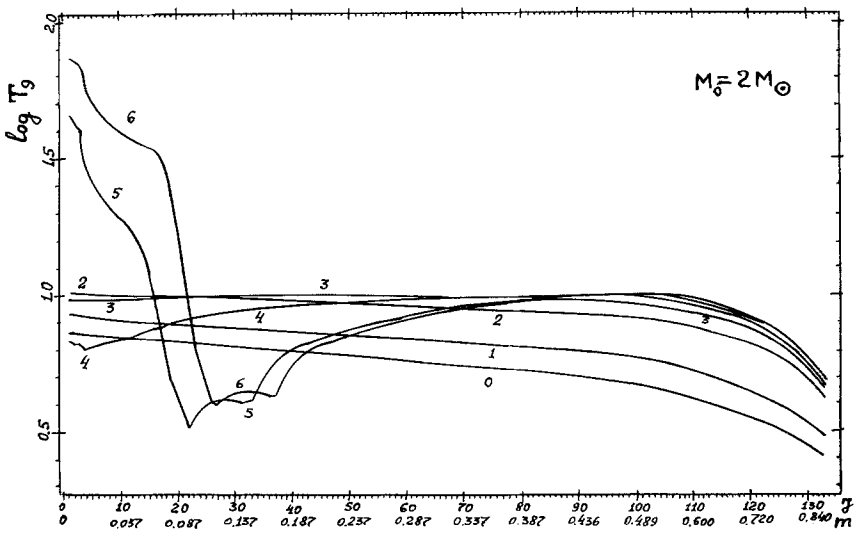

Fig. 2. Temperature versus Lagrangian coordinate at transparent stage of the collapse for the same moments of time as in Figure 1. The mass scale is also indicated under horizontal axis.

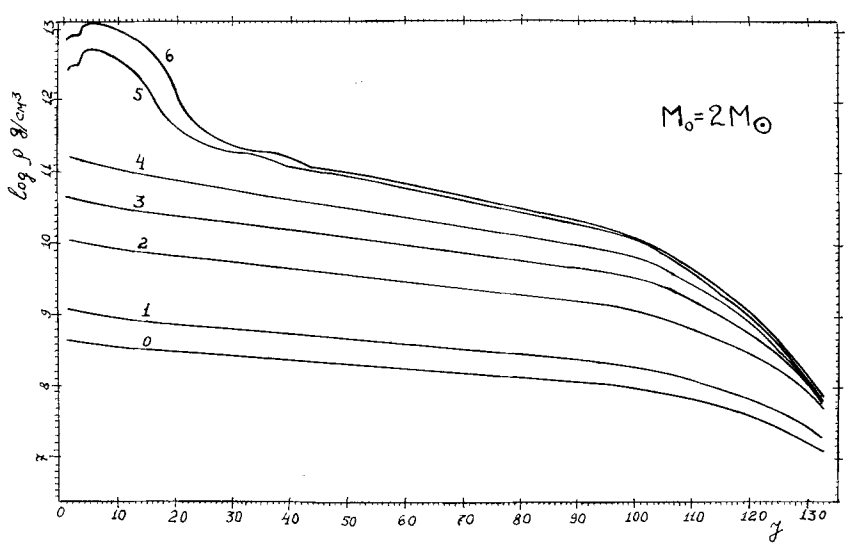

Fig. 3. Density versus Lagrangian coordinate at transparent stage of the collapse.

At the beginning of the collapse, the central temperature increases with the central density. When, however, the latter becomes greater than about 10^{10} g cm^{-3}, it begins to decrease (cf. the moments 2, 3, and 4 in Figures 1 and 2). The noticeable drop in temperature occurs in the central region of the collapsing star when an intensive neutronization begins at densities $\varrho \approx 3 \times 10^{11}$ g cm^{-3} (see Figure 1 and temperature distributions in the range of $J=20$–30 in Figure 2 for moments 5 and 6). This

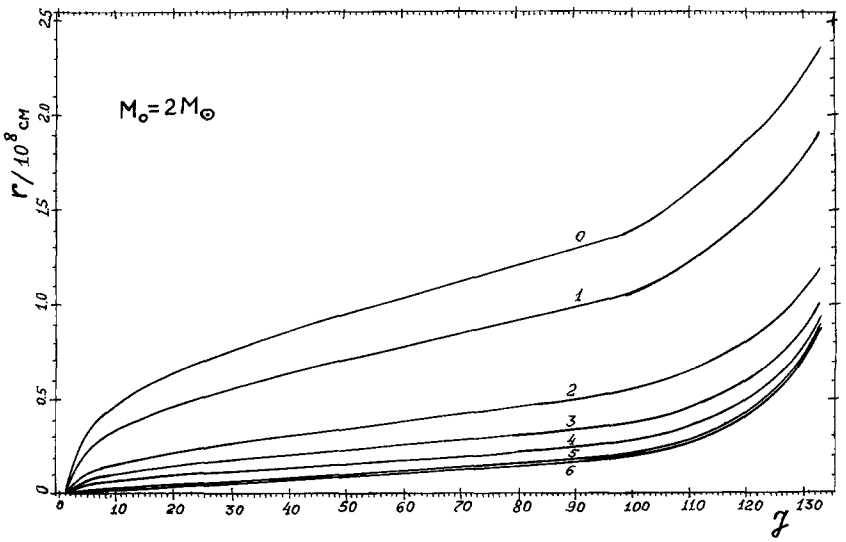

Fig. 4. Eulerian radius versus Lagrangian coordinate at transparent stage of the collapse.

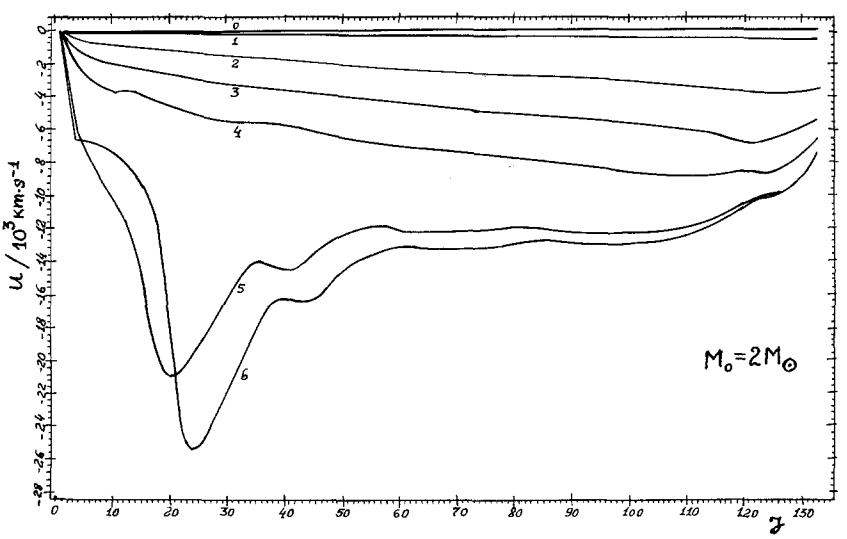

Fig. 5. Velocity versus Lagrangian coordinate at transparent stage of the collapse.

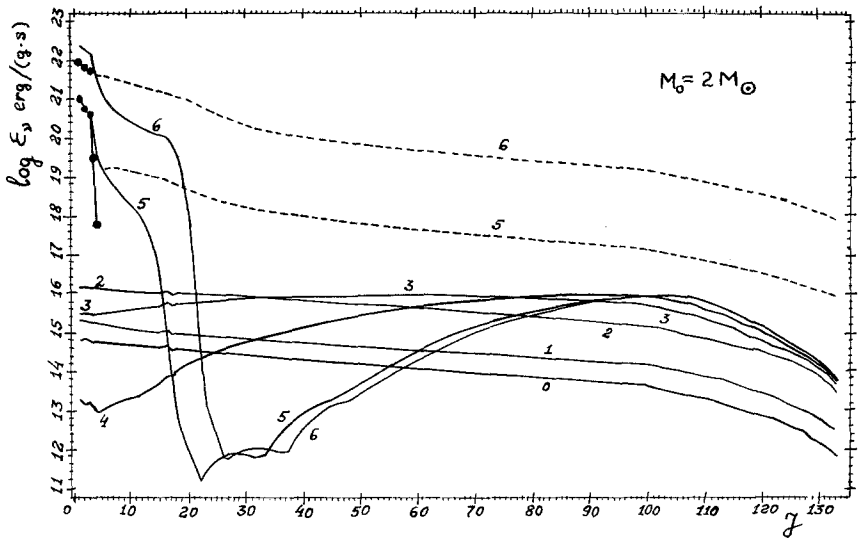

Fig. 6. Volume neutrino energy losses versus Lagrangian coordinate at transparent and semitransparent stages of the collapse (see text for details).

temporary decrease of temperature is accounted for by the appearance of a large number of free *non-degenerated* neutrons. As a result, the entropy reveals an inverse dependence on density – i.e., it begins to increase with density at constant temperature $(\partial S/\partial \varrho)_T > 0$ (Imshennik and Chechetkin, 1970). With thermodynamical inequality $(\partial S/\partial T)_\varrho > 0$ (Landau and Lifshitz, 1964) in mind, one can show the sign of the derivative $(\partial T/\partial \varrho)_S$ to be opposite to the sign of the derivative $(\partial S/\partial \varrho)_T$ and, therefore, the inequality $(\partial T/\partial \varrho)_S < 0$ is satisfied. This is the reason why the temperature decreases with increasing density under the conditions of *thermodynamic equilibrium* neutronization. When, for $\varrho \gtrsim 10^{12}$ g cm^{-3}, the neutronization is becoming complete, the entropy begins to decrease with increasing density at constant temperature and, therefore, the temperature begins to rise again in the course of the collapse. Besides, the mean neutrino-antineutrino 'optical' depth τ_ν is growing rapidly: at the moments 5 and 6, it already exceeds 0.001, and the volume neutrino energy losses in the central region of the collapsing star are now partly compensated due to the absorption of its own volume neutrino radiation. (See the discussion of Figure 6 below.) Thus a small, hot, and dense core is being formed in the central region of the collapsing star. The relative mass of this core is about $m/M_0 \approx 0.08$. The neutrino 'optical' depth of the core, $\tau_{\nu\,\mathrm{cor}}$, increases rapidly. Indeed, it takes $\tau_{\nu\,\mathrm{cor}}$ only $\sim 10^{-4}$ s after the moment 6 to exceed 1. Hence, the physical conditions inside the collapsing star, as given by distributions in Figures 2–6 at moment 6, just precede the rise of the 'neutrino core'.

Let us consider now the approximation of the kinetic equilibrium of the beta-processes of which use was made in our calculations. The fact that beta-processes are, in general, delayed to some extent leads to non-equilibrium character of the

neutronization with the resulting increase of entropy (Bisnovatyi-Kogan and Seidov, 1970; Nakazawa, 1973; Basko and Imshennik, 1975). The smaller the mass of a star, the greater the divergence of the neutronization from the kinetic equilibrium. When the mass of the star is close to the Chandrasekhar limit, the kinetics of the neutronization is the main feature to be taken into account in the calculations of the collapse. Basko and Imshennik (1975) thoroughly investigated the kinetics of the neutronization. They approximated the hydrodynamics of the collapse by a profile of the density distribution. However, the evolution of temperature was considered in full detail, taking into account the complex equation of state for the adequate mixtures of various iron-group nuclei.

According to Basko and Imshennik, the entropy increases noticeably as the nonequilibrium neutronization proceeds, even for the maximum value of the stellar mass 1.7 $M_\odot$ which was considered in their work. As a result, the temperature shows a slow but steady rise with density. Thus, the central temperature is somewhat underestimated in our calculations of the collapse of 2 $M_\odot$ star (the moments 3 and 4 in Figures 1 and 2). This underestimate is mainly due to an equilibrium character of neutronization adopted in our calculations. The approximate method of density profiles applied by Basko and Imshennik works well during the first phases of the collapse up to the violation of its homogeneity at moments 5 and 6 (Figure 1, 2, and 3). Indeed, Figures 3, 4, and 5 show that the collapse of the 2 $M_\odot$ star looks nearly homogeneous till the moment 4: the distribution of density in the central part of the collapsing star, for $J \lesssim 100$, $m/M_0 \lesssim 0.5$, retains approximately its initial shape as given by the polytropic structure of index $n=3$ and suffers a rather small deformation in the outer regions of the star. Therefore, it is not surprising that the results of Basko and Imshennik for the 1.7 $M_\odot$ star are in agreement with ours for 2 $M_\odot$ up to the moment 4. For example, the times of contraction from the central density of 10^{10} g cm^{-3} to 10^{11} g cm^{-3} are nearly the same; the central temperatures at the moments 1 and 2 are also in a quantitative agreement. The underestimate of the temperature in the vicinity of the stellar center in our calculations at moments 3 and 4 is, in any case, insignificant for subsequent development of the collapse, since the region with low temperature is rapidly heated up by the absorption of the neutrino radiation (see Figures 2 and 10).

Figure 6 shows the volume neutrino energy losses (full lines) versus the Lagrangian coordinate. For moments 5 and 6, the difference between energy deposition rate, $\varepsilon_{\nu d}$, and energy losses, ε_ν at the semi-transparent stage of the collapse (NI) is also given. This difference is represented in the form of $\log|\varepsilon_{\nu d}-\varepsilon_\nu|$; the dashed lines refer to the case of $\varepsilon_{\nu d}-\varepsilon_\nu>0$; and the case of $\varepsilon_{\nu d}-\varepsilon_\nu<0$ is marked by solid circles. According to Figure 6, the external layers of the star are heated up by partial absorption of neutrinos and antineutrinos radiated by the central region of the star. As a result, the temperature profile in the form of a step is created near the centre of the star (the moment 6).

At the transparent stage, the collapse of a 10 $M_\odot$ star proceeds nearly the same way as in the case of a 2 $M_\odot$ star. However, there is a difference: the heterogeneity of the

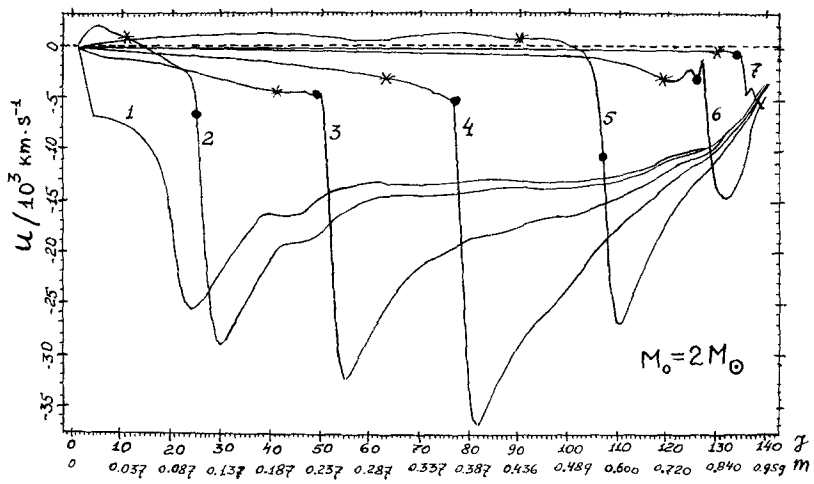

Fig. 7. Velocity versus Lagrangian coordinate at opaque stage of the collapse. The moments of time which correspond to integers 1–7 are listed in Table III. The symbols * and ● denote the position of the neutrino photosphere and boundary of the neutrino core, respectively.

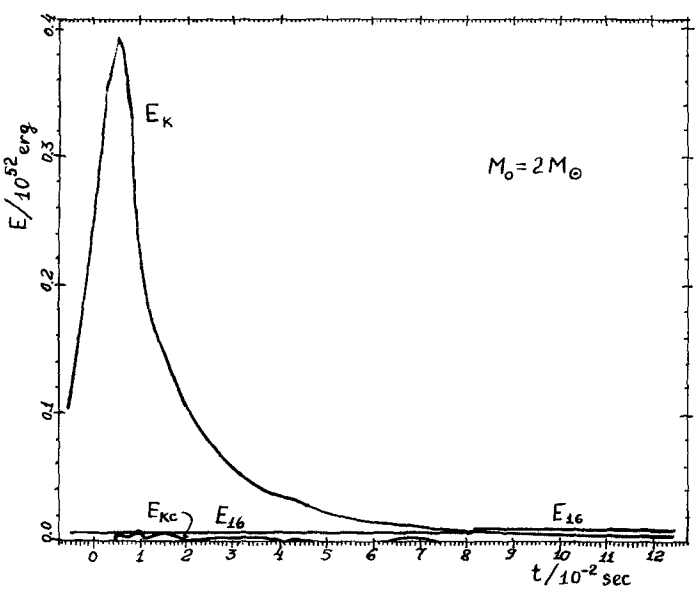

Fig. 8. Kinetic energy of the star, E_k, kinetic energy of the neutrino core, E_{kc}, and energy released due to oxygen burning, E_{16}, versus time.

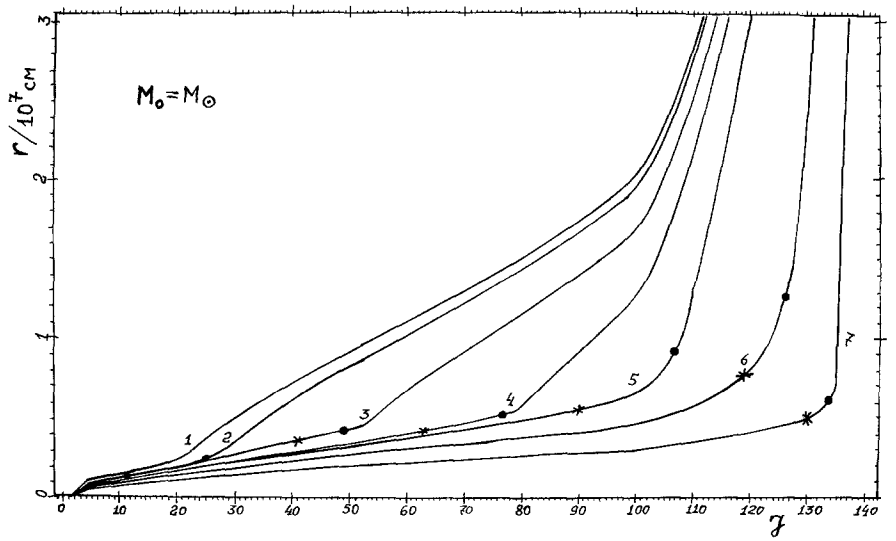

Fig. 9. Eulerian radius versus Lagrangian coordinate at opaque stage of the collapse.

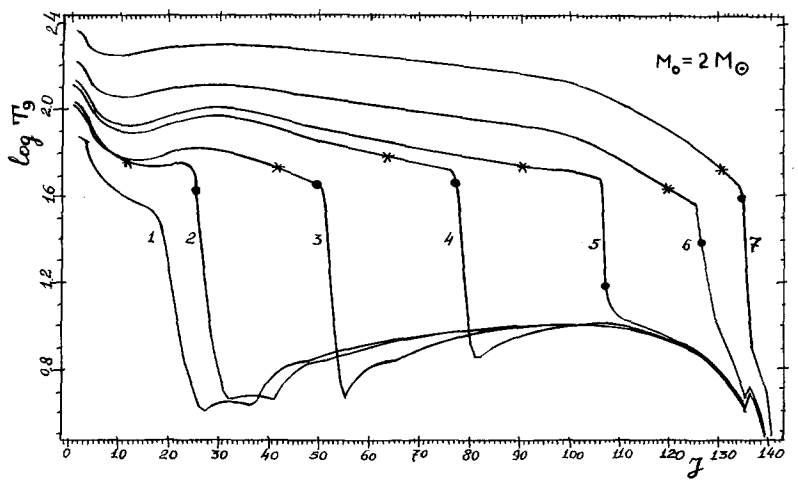

Fig. 10. Temperature versus Lagrangian coordinate at opaque stage of the collapse.

collapse manifests itself in a more violent form. This is accounted for by the adiabatic index in the case of a 2 $M_\odot$ star being close to the critical value of 4/3 in the relatively large central region of the star, while in the case of a 10 $M_\odot$ star, the large part of the star (excluding the small central core) has the adiabatic index about 5/3 just before the loss of stability. Moreover, in a 10 $M_\odot$ star the temperature is higher and the density is lower than in a 2 $M_\odot$ star and, therefore, the above-mentioned decrease of temperature with increase of density is absent. In spite of the more accurate treatment of the

collapse in our present calculations as compared with the work of Ivanova *et al.* (1969), the physical characteristics of the 10 $M_\odot$ star at the transparent stage of the collapse proved to be practically unchanged.

The properties of the collapsing stars of 2 $M_\odot$ and 10 $M_\odot$ just before the formation of the neutrino core are presented in Table II. From Table II it follows that, at the onset

TABLE II

The characteristics of the models of collapsing stars just before neutrino core rising

The total mass of the star	M_0	$2\,M_\odot$	$10\,M_\odot$
The central temperature	T_c	74.7×10^9 K	61.1×10^9 K
The central density	ϱ_c	7.21×10^{12} g cm^{-3}	5.24×10^{12} g cm^{-3}
The total gravitational energy	E_g	-2.15×10^{52} erg	-7.44×10^{52} erg
The total internal energy	E_{in}	1.79×10^{52} erg	5.75×10^{52} erg
The total kinetic energy	E_k	0.32×10^{52} erg	1.47×10^{52} erg
The total energy lost by neutrino radiation	E_ν	1.0×10^{49} erg	7.3×10^{50} erg
The total energy released due to oxygen burning	E_{16}	7.2×10^{48} erg	4.4×10^{50} erg
The rate of energy generation due to oxygen burning (thermonuclear luminosity)	L_{16}	3.75×10^{48} erg s^{-1}	6.04×10^{50} erg s^{-1}
The total neutrino-antineutrino luminosity	L_ν	1.1×10^{52} erg s^{-1}	6.7×10^{53} erg s^{-1}
The contribution of URCA process in L_ν	$\frac{L_\nu^{\mathrm{URCA}}}{L_\nu}$	0.99993	0.9996

of neutrino opacity, the values of central temperature and density depend but weakly on the mass of the collapsing star. The last line of Table II shows that the contribution of URCA-processes to overall neutrino luminosity is overwhelming – though at the very beginning of the collapse, when the star is at the boundary of mechanical stability, the main contribution to neutrino luminosity is due to the Universal Fermi Interaction (NI).

3. The Opaque Stage of the Collapse

The development of the collapse is violently changed with the onset of neutrino opacity in the central region of a collapsing star. In this case, the transport of energy within the neutrino core has to be described in terms of neutrino heat conductivity equations which include also another diffusion equation for the transport of lepton charge (Imshennik and Nadyozhin, 1972). The transport of momentum in the framework of neutrino heat conductivity theory is taken into account by adding the pressure of

thermodynamically equilibrium neutrino-antineutrino gas to that of matter; the specific energy is also a sum of material and neutrino-antineutrino energy. Besides, an absorption of neutrinos and antineutrinos escaping from the neutrino photosphere by the envelope which surrounds the neutrino core becomes important.

Figure 7 shows the velocity versus Lagrangian coordinate for a 2 $M_\odot$-model at various times listed in Table III. Figures 7 to 15 correspond to the case calculated with the neglect of the radiation of muon neutrinos. The effect of muon neutrinos on the

TABLE III

The moments of time for Figures 7 and 9–15. (The time is measured in the same way as in Table I)

The integers labeling the curves in Figures 7 and 9–15	The number of calculated time steps	Time in seconds
1	16 600	0.001 91
2	16 650	0.002 48
3	16 950	0.004 28
4	17 250	0.006 48
5	17 700	0.010 6
6	20 650	0.036 8
7	39 150	0.125

gravitational collapse will be discussed in the following section. The rise of the neutrino core is followed by the appearance of a strong shock-wave which separates the neutrino core from the collapsing envelope (Figure 7). The matter of the envelope is accelerated up to very high velocities: the maximum speed of the fall amounts to 37 000 km s^{-1} (0.12 c) at the moment 4 and proves to be only ~ 1.5 times smaller than the limiting speed of free fall $\sqrt{(2\,Gm/r)}$, and several times as large as the speed of sound. The kinetic energy of infalling matter is mostly converted into thermal energy when matter passes through the shock.

As a result, temperature behind the shock jumps to the value of $T_9 = 40$–50 (Figure 10) and thus the conditions for neutrino heat conductivity are being created. Incident matter is also heated before the shock by the diluted neutrino radiation escaping from the neutrino photosphere. However, this heating is sufficient only to compensate the energy losses due to volume neutrino radiation. Consequently, the motion of matter before the shock is found to be nearly adiabatic, and the increase of the neutrino core mass is mainly allowed for by the heating of matter by the shock wave. At the moment 6, a large supply of kinetic energy accumulated in collapsing matter during the transparent stage of the collapse is found to be nearly all converted into heat. This gives rise to a quick (for ~ 0.04 s) increase of the mass of the neutrino core to the value of

$M_\nu/M_0 \approx 0.8$. Figure 8 shows the total kinetic energy of the collapsing star, the kinetic energy of the neutrino core, and the energy released due to oxygen burning versus time. As follows from Figures 7 and 8, with a growth of its mass, the neutrino core suffers pulsations of small amplitude. At moment 7, the pulsations come to an end; the velocity of matter before the shock decreases considerably and, therefore, the growth of the neutrino core mass is highly decelerated. Indeed, between the moments 6 and 7 during the time of 0.088 s, the mass of the neutrino core increases only from 0.8 $M_\odot$ to 0.89 $M_\odot$.

The gravitational collapse comes now in a prolonged stage of envelope accretion onto a hot neutron star originating in the center of the collapsing star. This stage of the collapse evolves in close agreement with the results obtained by Zel'dovich *et al.* (1972) for the accretion onto a neutron star. From Figure 9 it follows that the Eulerian radii of the neutrino core and the neutrino photosphere begin to decrease slowly at the accretion stage of the collapse. On the contrary, at the preceding stage of rapid growth of the neutrino core they show a noticeable increase. This is accounted for by the fact that the energy losses due to neutrino radiation from the surface of the neutrino core at the stage of accretion begin to exceed the energy input from accreting flow; while at the stage of neutrino core growth a converse situation is encountered. Thus, the neutrino core is gradually losing its thermal and gravitational energy, and contracts slowly in the course of accretion. According to Figures 10 and 11, the temperature and the density at the boundary of the neutrino core as well as at the neutrino photosphere begin to increase in the stage of accretion (cf. T- and ϱ-distributions at moments 6 and 7).

Figure 12 shows the distribution of mean neutrino-antineutrino optical depth τ_ν. The position of the neutrino photosphere corresponds to $\tau_\nu = 0.2$–0.6 and the

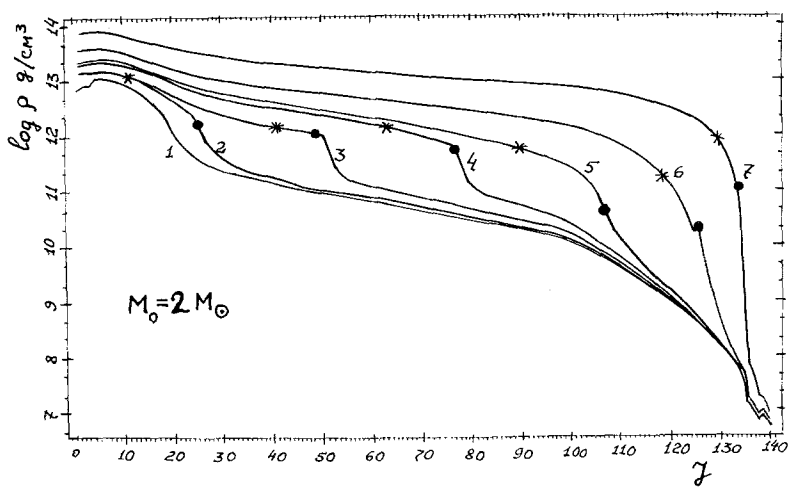

Fig. 11. Density versus Lagrangian coordinate at opaque stage of the collapse.

boundary of the neutrino core is maintained in accordance with NI in the range of $0.01 < \tau_\nu \lesssim 0.03$.

Figures 13, 14, and 15 illustrate the distribution of the neutrino and electron chemical potentials ψ_ν and ψ_e (in units of kT), and neutron-to-proton ratio $\theta = n_n/n_p$, over the neutrino core. In the first moments after the formation of the neutrino core, ψ_ν is negative over the core (i.e., antineutrino density exceeds neutrino density). This is

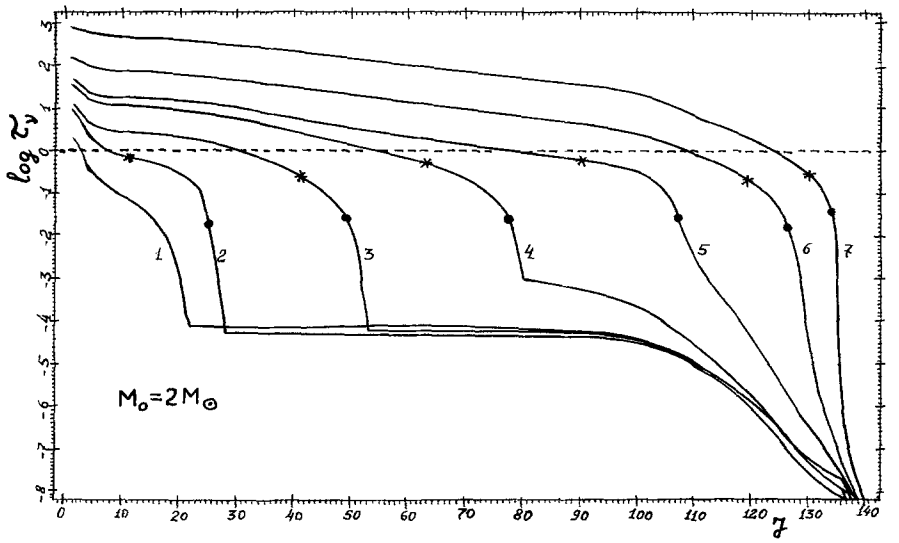

Fig. 12. Neutrino optical depth versus Lagrangian coordinate at opaque stage of the collapse. The dashed horizontal line indicates the level $\tau_\nu = 1$.

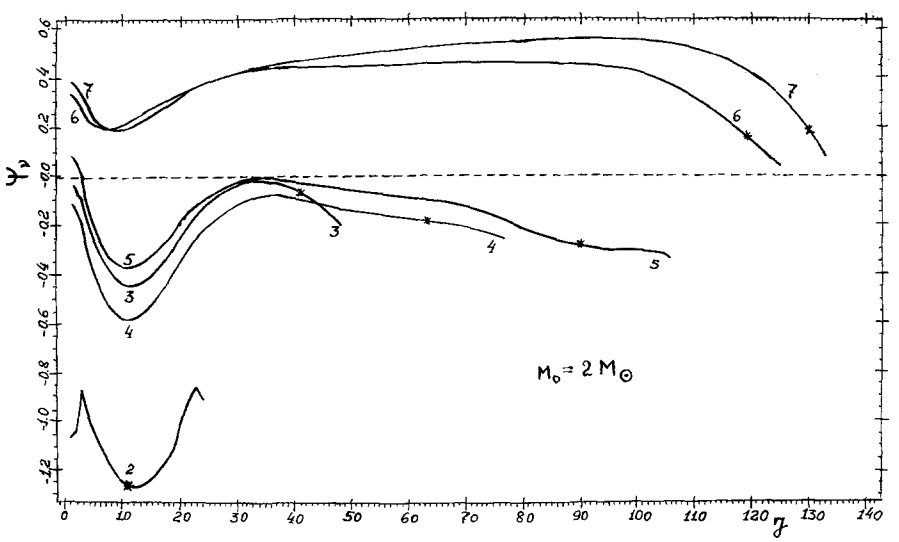

Fig. 13. Neutrino chemical potential in neutrino core versus Lagrangian coordinate.

due to the fact that matter near the stellar center consists of almost pure neutrons ($\theta \approx 100$) just after the neutrino core rise. The onset of neutrino opacity invokes the operation of the reactions of neutrino and antineutrino absorption which lead to a gradual reduction of θ – a process inverse to neutronization. As a result, at the first phase of neutrino core existence (moments 2 to 5) the radiation of antineutrinos from the surface of the core exceeds that of the neutrinos. Then after the moment 7, θ attains

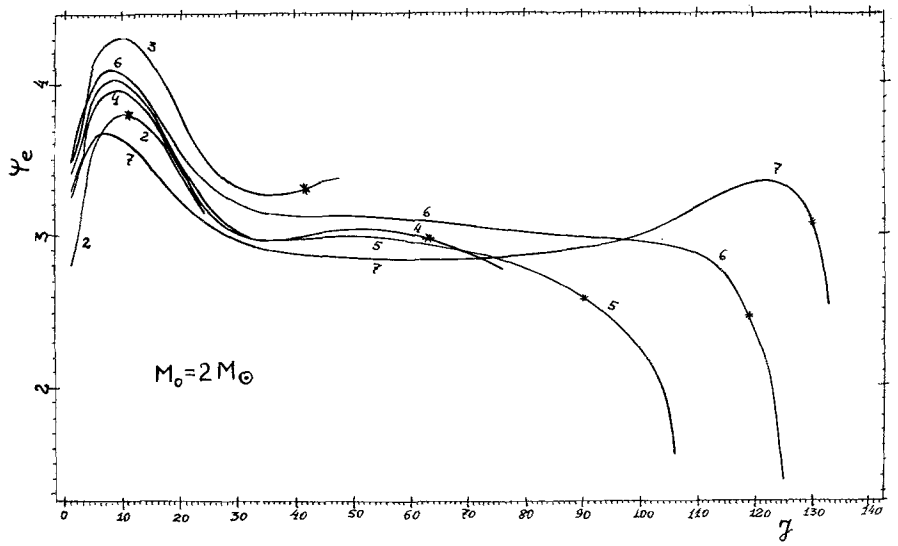

Fig. 14. Electron chemical potential in neutrino core versus Lagrangian coordinate.

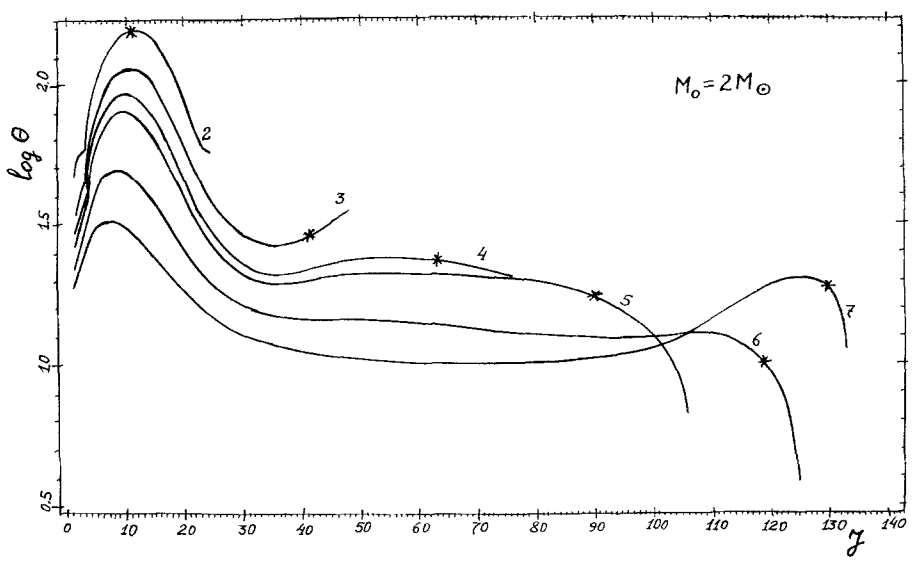

Fig. 15. Neutron-to-proton ratio, θ, in neutrino core versus Lagrangian coordinate.

a nearly steady-state value of $\theta = 10$–20 inside the core (see the moments 6 and 7 on Figure 13) and the surface of the core now radiates neutrinos in preference to antineutrinos. However, the difference is not very large, since the value of ψ_ν is found to be close to 0 at the surface of the neutrino core.

In Figure 10, one can notice an inversion of temperature distribution for Lagrangian coordinate J varying between 10 and 25 and for the time being somewhat later than moment 2. As before, however, the energy continues to be transported by neutrino heat conductivity in this region in the direction from the centre to the surface, since the overall energy flux is accounted for not only by the temperature gradient but also by the gradient of neutrino chemical potential (Imshennik and Nadyozhin, 1972; Mazurek, 1974). The inverse temperature gradient is found to be fully compensated by a steep gradient of ψ_ν (Figure 13). It should be noted that the gradients of ψ_ν and T contribute equally (in order of magnitude) to the neutrino energy flux and the lepton charge flux for all modes of the gravitational collapse which we have calculated for the stars with masses of 2 $M_\odot$ and 10 $M_\odot$.

The collapse of the 10 $M_\odot$ star becomes relativistic just after the rise of the neutrino core. In 0.3 s after the moment when $\tau_\nu = 0.001$, the neutrino core contains about 6 $M_\odot$ and has the dimensions of about 20 km; its neutrino optical depth attains the value of 10^6! The maximum value of the ratio r_g/r is reached near the surface of the neutrino core and amounts to 0.9. It is quite clear that these conditions require for GTR effects to be taken into account in full-scale hydrodynamics and neutrino heat conductivity. Therefore, the calculations of the 10 $M_\odot$ star collapse were terminated at this moment.

4. The Role of Muon Neutrinos

The calculations of 2 $M_\odot$ star collapse described above does not allow for the effects connected with muon neutrinos. The volume energy losses due to muon neutrinos become important for temperatures $T_9 \geqslant 150$–200. However, the central regions of the collapsing star soon prove to be opaque with respect to muon neutrinos when temperature approaches the value of $T_9 = 300$–350. A special variant of a 2 $M_\odot$ star collapse was calculated to reveal the effects caused by muon neutrinos. In accordance with NI, the muon neutrino opacity was taken into account by inserting a correction factor $\exp(-\tau_{\nu\mu})$ in the law of the volume muon neutrino energy losses; $\tau_{\nu\mu}$ being the muon neutrino 'optical' depth of the star. The results of these calculations are presented in Figures 16 and 17. Figure 16 shows the velocity distribution over the external part of the star ($60 \leqslant J \leqslant 151$) and Figure 17 illustrates the density distributions over the internal part of the star ($1 \leqslant J \leqslant 130$) at various times. Till the moment 4, the collapse is practically unaffected by radiation of muon neutrinos. Then, as soon as the central temperature begins to exceed 150×10^9 K, the energy losses due to muon neutrinos give rise to an additional rapid collapse which manifests itself in a sharp acceleration of contraction (see the velocity distribution in Figure 16 at moment 5), followed by the increase of central density up to 2×10^{15} g cm^{-3} (Figure 17) and

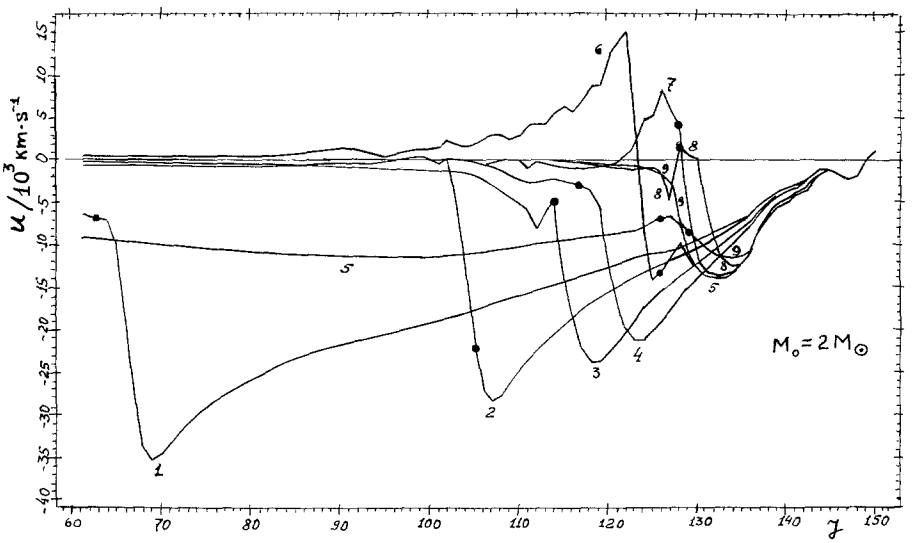

Fig. 16. The influence of muon neutrino radiation on velocity distribution in the collapsing star. The moments of time corresponding to numbers 1–9 are presented in Table IV.

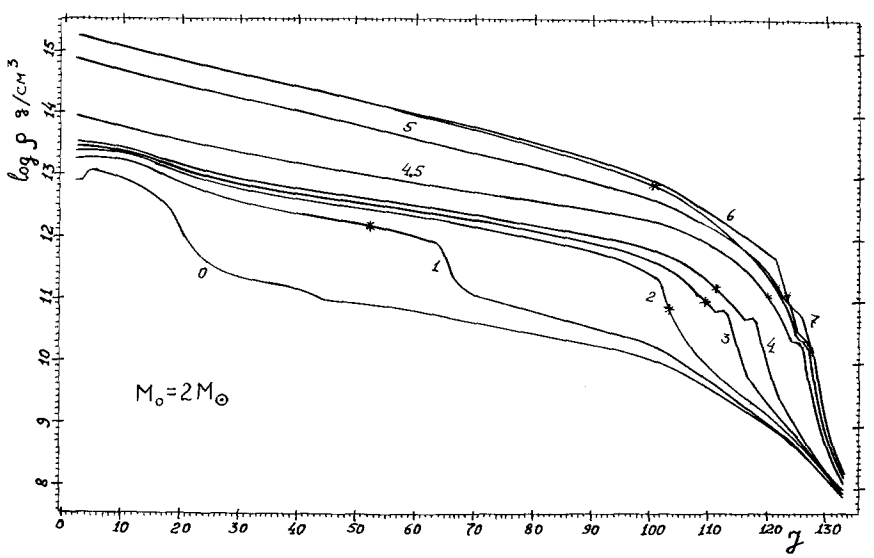

Fig. 17. The influence of muon neutrino radiation on density distribution in collapsing star.

central temperature up to 400×10^9 K. All this readjustment of the collapse leads ultimately to a considerable increase in muon neutrino optical depth $\tau_{\nu\mu}$. At the moment 6, $\tau_{\nu\mu}$ approaches the value of about 50–100, and the energy losses by means of muon neutrinos vanish, since $\exp(-\tau_{\nu\mu})$ becomes too small. Therefore, after the moment 6, an additional collapse induced by muon neutrinos proves to be attenuated

almost as quickly as it developed before. This is clearly illustrated by close coincidence of density distributions for $J<100$ at the moments 6 and 7 (Figure 17). However, the additional collapse due to muon neutrino radiation appears to be able to generate a powerful outgoing shock wave arising from the hydrodynamical recoil on the core (see the moment 6 in Figure 16).

In the course of subsequent propagation, the shock is gradually decelerated owing to the collision with the collapsing envelope and the intensive radiation of energy from the surface of the neutrino core (cf. moments 7 and 8 in Figure 16). The disturbance caused

TABLE IV

The moments of time for Figures 16 and 17. (The time is measured in the same way as in Tables I and III)

The numbers labeling the curves in Figures 16 and 17	The number of calculated time steps	Time in seconds
0	16 600	0.001 91
1	17 100	0.003 50
2	17 600	0.007 54
3	18 100	0.013 0
4	18 600	0.017 8
4.5	20 600	0.032 9
5	21 600	0.037 1
6	22 600	0.038 5
7	23 600	0.039 9
8	26 600	0.044 1
9	30 600	0.049 6

by the radiation of muon neutrinos ultimately fades away, and the collapse enters in the stage of slow accretion (moment 9 in Figure 16) which proceeds nearly in the same way as in the case when the muon neutrinos are neglected. The method of allowing for the opacity with respect to muon neutrinos by means of factor $\exp(-\tau_{\nu\mu})$ is quite similar to that used earlier by Ivanova *et al.* (1969) for accounting of opacity with respect to electron neutrinos. A comparison of present calculations, carried out with the aid of the equations of neutrino heat conductivity for electron neutrinos, with the results obtained by Ivanova *et al.* (1969), indicates that the method of $\exp(-\tau)$ makes the neutrino energy losses cut off too rapidly. This cut-off leads to an abrupt readjustment of the velocity distribution over the collapsing star. Therefore, the outgoing shock wave generated in the case with muon neutrinos being taken into account is found to be exclusively a consequence of the approximate treatment of the muon neutrino opacity. Nevertheless, this shock-wave enables us to draw a certain conclusion about the stability of the stellar envelope with respect to an ejection of matter (Section 5).

The discovery of neutral currents in the weak interaction has resulted in the mass opacity with respect to muon neutrinos being of the same order of magnitude as that for the electron neutrinos (Weinberg, 1974). Under these circumstances, the transport of energy by muon neutrinos in neutrino heat-conductivity theory could have been accounted for effectively by multiplying the energy flux due to electron neutrinos with a factor of the order of unity. However, it is quite obvious that such modification of the neutrino heat conductivity coefficients is hardly capable of changing considerably the results of calculations carried out without muon neutrinos being taken into account. Therefore, we believe the case calculated without the muon neutrinos to be quite real – in the sense that the self-consistent consideration of muon neutrinos will not apparently change the qualitative side of the gravitational collapse as compared with the case when the muon neutrinos are neglected.

5. The Oxygen Burning Induced by Gravitational Collapse and the Problem of Envelope Ejection

The oxygen burning induced by the gravitational collapse of the 2 $M_\odot$ and 10 $M_\odot$ stars proceeds in a steady, nonexplosive manner. Oxygen burns up step by step, layer by layer, as it collapses onto the collapsed central core. One can recognize the consequences of oxygen burning in small local changes of temperature, density (Figure 1), and velocity of collapsing matter (Figure 16 at $J=136$–140). Such a regime of oxygen burning occurs because the oxygen envelope does not impinge onto the collapsed core at once as a whole, but is drawn instead towards it in a slow quasi-steady accretion flow. Under such conditions, the overall amount of nuclear fuel which could have been stored in an extended stellar envelope is found to be rather unimportant for the establishment of the quasi-steady accretion flow.

The burning of the remnants of nuclear fuel in the envelope during the gravitational collapse has been also studied by Barkat *et al.* (1975), with due allowance for various nuclear species in the intermediate range of atomic weights from light nuclei to those of the iron-group. Calculations for various initial masses of the iron core disclosed that nuclear burning induced by the gravitational collapse is also nonexplosive.

According to our calculations, the heating of the envelope due to escape of neutrinos from a neutrino photosphere (the envelope consisting of oxygen is heated up mostly by neutrino-electron scattering) failed to induce the detonation of oxygen. Figure 18 shows the total energy radiated by the surface of the neutrino core, $\mathscr{E}_{\nu c}$, the energy, $\mathscr{E}_{\nu d}$, absorbed by the envelope (deposited energy), and the energy, $\mathscr{E}_{\nu V}$, lost owing to volume radiation versus time. It can be noted that the excess of the deposited energy $\mathscr{E}_{\nu d}$ over the volume energy losses $\mathscr{E}_{\nu V}$ is relatively small. Thus the role of the deposited energy is mainly to compensate the volume energy losses. The results of the calculations discussed above leads us to a conclusion that *the deposited energy is incapable not only of causing an ejection of matter, but also of igniting the nuclear fuel in the envelope.*

A large margin of stability of the envelope with respect to ejection follows also from

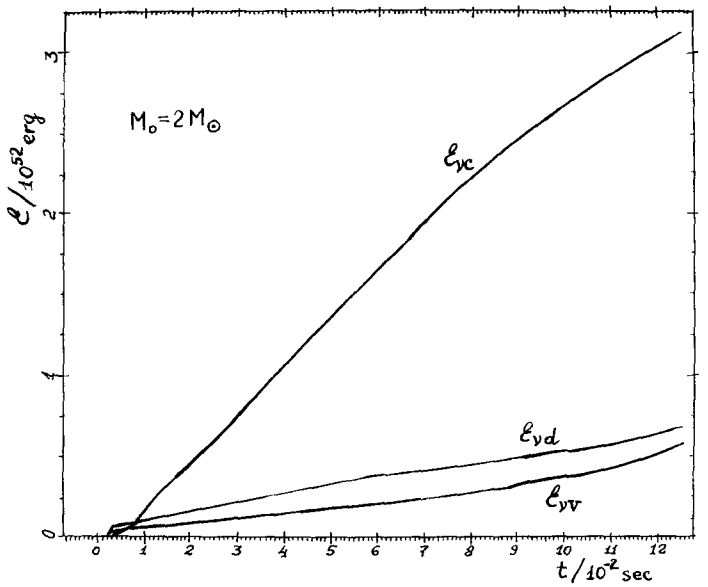

Fig. 18. Energy radiated from the surface of the neutrino core, $\mathcal{E}_{\nu c}$, deposited energy, $\mathcal{E}_{\nu d}$, and energy lost due to volume neutrino radiation, $\mathcal{E}_{\nu\nu}$, as functions of time.

the fact that a powerful shock-wave, resulting from the abrupt cut-off of the muon neutrino radiation, failed to eject even a small fraction of the mass of the envelope.

There remains yet a question of the influence of the neutrino-nuclear coherent scattering on the motion of stellar envelope to be studied. It will be discussed in my next paper.

6. Conclusions

The results obtained in the present paper can be summarized as follows. The collapse of iron–oxygen stars of masses 2 $M_\odot$ and 10 $M_\odot$ begins as a result of thermal dissociation of iron-group nuclei into alpha-particles and free nucleons. When the central density becomes as high as $(0.5\text{–}1) \times 10^{13}$ g cm^{-3} (the corresponding central temperature is found to be about $(60\text{–}75) \times 10^9$ K) the neutrino 'optical' depth of the collapsing star approaches 1. Thus, a small core, opaque with respect to neutrinos and antineutrinos, is formed at the centre of the star. Just after its formation, this 'neutrino core' increases its mass rapidly owing to a conversion of kinetic energy of incident matter into heat when this matter passes through the shock front. During this phase of the collapse, the neutrino core is growing both in mass and dimensions. After most of its kinetic energy becomes exhausted, the collapse enters the stage in which the remaining outermost layers of the envelope are accreted onto the neutrino core. The accretion proceeds in a quasi-stationary manner, and available nuclear fuel (oxygen) is being consumed steadily. The heating of the envelope due to neutrinos and antineutrinos radiated by

the neutrino core (so-called neutrino energy deposition) is of the same order of magnitude as the cooling of the accreting envelope by its own volume neutrino energy losses. The models of iron–oxygen star collapse, discussed above, does not give any evidence in favour of either the neutrino energy deposition or the oxygen burning being capable of ejecting any part of the stellar envelope.

Acknowledgement

The author would like to express his gratitude to V. S. Imshennik for numerous helpful discussions at all stages of this research.

References

Barkat, Z., Rakavy, G., Reiss, Y., and Wilson, J. R.: 1975, *Astrophys. J.* **196**, 633.

Basko, M. M. and Imshennik, V. S.: 1975, *Astron. Zh.* **52**, 469. Translation in English: *Soviet Astron. – AJ* **19**, 286.

Bisnovatyi-Kogan, G. S. and Seidov, Z. F.: 1970, *Astron. Zh.* **47**, 139. Translation in English: *Soviet Astron. – AJ* **14**, no 1.

Ivanova, L. N., Imshennik, V. S., and Nadyozhin, D. K.: 1969, *Nauch. Inform. Astron. Sovieta U.S.S.R. Acad. Sci.* **13**, 3.

Imshennik, V. S. and Chechetkin, V. M.: 1970, *Astron. Zh.* **47**, 929. Translation in English: *Soviet Astron. – AJ* **14**, 747.

Imshennik, V. S. and Nadyozhin, D. K.: 1972, *Zh. Eksp. Teor. Fiz.* **63**, 1548. Translation in English: *Soviet Phys. – JETP* **36**, 821.

Landau, L. D. and Lifshitz, E. M.: 1964, *Statistical Physics*, Nauka, Moscow.

Mazurek, T. J.: 1974, *Nature* **252**, 287.

Nadyozhin, D. K.: 1975, Preprint IAM No 98. English version in *Astrophys. Space Sci.* **49** (1977), 399.

Nakazawa, K.: 1973, *Progr. Theor. Phys.* **49**, 1932.

Weinberg, S.: 1974, *Rev. Mod. Phys.* **46**, 255.

Zel'dovich, Ya. B., Ivanova, L. N., and Nadyozhin, D. K.: 1972, *Astron. Zh.* **49**, 253. Translation in English: *Soviet Astron. – AJ* **16**, 209.